ARTICLE
Journal of Cellular Biochemistry 114:2624–2636 (2013)

Journal of Cellular Biochemistry

Characterization of Human Dental Pulp Cells-Derived Spheroids in Serum-Free Medium: Stem Cells in the Core

Li Xiao* and Takeki Tsutsui

Department of Pharmacology, The Nippon Dental University, School of Life Dentistry at Tokyo, 1-9-20 Fujimi, Chiyoda-ku, Tokyo, 102-8159, Japan

ABSTRACT

Spheroid models have led to an increased understanding of differentiation, tissue organization and homeostasis. In the present study, we have observed that under a serum-free medium, human dental pulp cells (DPCs) spontaneously formed spheroids, and could survive over 15 weeks. To characterize these spheroids, we investigated their dynamics, microenvironment, cell distribution, molecular profiles, and neuronal/osteogenic potential. Cell tracking assay showed that cells inside the spheroids have very slow cycling. Although the spheroids had hypoxia microenvironments, there were not any massive cell die-offs even after long-term cultivation. Whole mount immunofluorescence staining and histological analysis showed a distribution of stem cells in the central/intermediate zones of spheroids. qRT-PCR analysis demonstrated that the expression of stemness markers *NANOG*, *TP63*, and *CD44* in the spheroids were much higher than within the monolayer cultures. Gene expression levels of neural markers *CDH2*, *NFM*, *TUBB3*, and *CD24* in the spheroids were much higher than the monolayer DPCs and increased in a culture time-dependent manner. Without any neural induction, spheroid-derived cells spontaneously converted into neuron-like cells with positive staining of neural markers HuC/D and P75 under the serum-free medium for about 2 weeks. When the spheroids were transferred into osteogenic medium, they rapidly differentiated into osteo/odontogenic cells, especially the central original cells. Compared to the monolayer DPCs, mineralization in spheroids were significantly increased. This spheroid model offers a study tool to explore the molecular bases of stem cell homeostasis and tissue organization, and can be wildly used for nerve tissue and bone regeneration. J. Cell. Biochem. 114: 2624–2636, 2013.

KEY WORDS: DENTAL PULP STEM CELLS; SPHEROID; NEURANAGENESIS; OSTEOGENESIS

For stem cell research, the two-dimensional (2D) monolayer cell culture systems provide efficient ways to identify stem cells and test their properties, such as multipotency, growth rate, and life span. However, monolayer culture systems have limitations in representing the in vivo cellular environment and cell behaviors. For example, in vivo adult stem cells such as neural stem cells reside in niches characterized by hypoxia and low abundance of nutrients, both of which the monolayer culture systems have difficulty to provide [Simon and Keith, 2008; De Filippis and Delia, 2011; Mannello et al., 2011; Suda et al., 2011]. Additionally, adult stem cells are characterized by slow or infrequent cycling in vivo whereas they usually possess high proliferative capacities when being cultured as monolayer cells in vitro [Cotsarelis et al., 1989; Fortunel et al., 1998; Nakamura et al., 2007].

In contrast to monolayer culture systems, the three-dimensional (3D) spheroid culture system represents a unique opportunity to reflect in vivo situations of cells. The spheroid models were first developed in tumor biology. The multicellular tumor spheroids not only displayed in vivo anti-tumor drug responses but also exhibited numerous pathophysiological features of tumor nodules and reproduced the tumoral microenvironment [Desoize et al., 1998; Santini and Rainaldi, 1999; Bates et al., 2000]. In embryological studies, the spheroid models are defined as embryoid bodies of both pluripotent and committed stem cells that can organize in a developmental-specific manner and give rise to mature cells from any differentiation lineage [Marga et al., 2007]. For adult stem cells research, 3D spheroid culture platforms showed improved differentiation efficiency of bone marrow mesenchymal stem cells [Wang et al., 2009], and preserved the viability and developmental plasticity of adipose stem cells even under defined, serum-free media conditions [Kapur et al., 2012]. In contrast, for normal fibroblasts, when they were forced into spheroid formation they did not proliferate but underwent cell death and decomposed after 120 h of incubation [Vaheri et al., 2009].

Grant sponsor: Japan Society for the Promotion of Science (JSPS); Grant numbers: 21890267, 23592903.
*Correspondence to: Dr. Li Xiao, Department of Pharmacology, The Nippon Dental University, School of Life Dentistry at Tokyo, 1-9-20 Fujimi, Chiyoda-ku, Tokyo 102-8159, Japan. E-mail: xiaoli@tky.ndu.ac.jp
Manuscript Received: 22 April 2013; Manuscript Accepted: 11 June 2013
Accepted manuscript online in Wiley Online Library (wileyonlinelibrary.com): 21 June 2013
DOI 10.1002/jcb.24610 • © 2013 Wiley Periodicals, Inc.

Human adult dental pulp cells (DPCs) originate from neural crest derived ectomesenchyme. DPCs also known as dental pulp stem cells because they exhibit multipotency under inductive conditions in vitro, and can form ectopic pulp-dentin like tissue complexes when they have been transplanted into immunocompromised mice [Gronthos et al., 2000; Huang et al., 2009]. Due to their common embryonic origin with the nervous system which also derived from neural crest, DPCs express neural crest-associated markers and can be differentiated into functional neurons under neural inductive conditions both in vitro and in vivo [Arthur et al., 2008; Abe et al., 2012]. Moreover, DPCs have potential to differentiate into other lineages: such as osteo/odontogenic, chondrogenic, adipogenic, and myogenic under specific differentiation mediums [Huang et al., 2009]. Thus multipotent DPCs are an attractive source for regenerative therapies, such as neural and osteogenic tissue regeneration.

Nevertheless, current culture method for DPCs is still dependent on fetal calf serum or human plasma-based monolayer culture systems. Due to serum and plasma contain undefined factors that limit their clinical use, serum-free culture media has been used for maintaining DPCs [Ishkitiev et al., 2012]. However it is unclear how DPCs behave under three-dimensional and serum-free conditions. (1) Do DPCs-derived spheroids survive for a long period of time or die quickly the same as the normal fibroblasts? (2) Do stem cells exist in the spheroids? Do they provide the microenvironment for stem cells, such as hypoxia? (3) Do cell rate, gene expression and multipotency change throughout the culture period? To answer these questions, we designed a series of experiments to test the above-mentioned subjects and their time-dependent changes in DPCs-derived spheroids under a serum-free condition.

MATERIALS AND METHODS

MATERIALS

General chemicals were purchased from Sigma-Aldrich (Tokyo, Japan), tissue culture medium from Invitrogen, Inc. (Tokyo, Japan) and tissue culture plastic from Corning Costar Ltd (NY), unless otherwise stated.

CELL CULTURE

To obtain human DPCs, lower third molars were got from adults (17–40 years old) at the Nippon Dental University Hospital at Tokyo under approved guidelines set by the Committee of Ethics, the Nippon Dental University School of Life Dentistry at Tokyo. DPCs from each donor were separated from the tooth and cultured in the maintenance medium (Table I) according to the previous report [Gronthos et al., 2000; Xiao and Tsutsui, 2012].

NDUSD-1 and Pelt cells were obtained and maintained as our previous reports [Tsutsui et al., 2002; Kubo et al., 2010].

SPHEROID FORMATION

Cells (1×10^6 cells/ml) were seeded into the regular culture flask or plate in KSR-medium containing 15% KnockOut™ Serum Replacement (Gibco, 10828-028) (Table I). For DPCs, the spheroids will form 24 h later.

TABLE I. Different Culture Media Used in the Study

Medium	The main ingredients
KSR-medium	MEM-α and 15% knock out serum replacement
Maintenance medium	MEM-α, 20% FBS, 1%GlutaMAX™ Supplement (Gibco), and 50 μM ascorbic acid 2-phosphate
Osteogeinc medium	MEM-α, 10% FBS, 1% GlutaMAX™ Supplement (Gibco) 50 μM ascorbic acid 2-phosphate, 0.1 μM dexamethasone, and 10 mM beta-glycerophosphate

OSTEOGENIC DIFFERENTIATION

Cells (1×10^6 cells/ml) or spheroids (10–20 spheroids/ml) were seeded in maintenance medium. When the monolayer cells reached 100% confluence, medium were changed to osteogenic medium (Table I). The cultures were further cultivated for another 2 weeks. The control cells were using the maintenance medium.

CELL TRACKING ASSAY

DNA in living cells and tissues was labeled with NucBlue® Live ReadyProbes™ Reagent (Hoechest 33342) (R37605, Invitrogen, Inc.). Ready-to-use liquid formulation of high-purity Hoechst 33342 was added to culture samples and incubated for 30 min. After washed two times with culture media, samples were further cultivated for about 4 weeks and observed with a confocal laser scanning microscopy (LSM 700, Carl Zeiss Microscopy Co., Ltd) every week. To observe the dynamics of cell division, we took time-lapse videos for about 72 h.

Membrane in living cells was labeled with PKH26 (PKH26GL, Sigma) according to the product information. Briefly, about 2×10^7 single cells were suspended in Diluent C (G8278, Sigma) and stained with PKH26 at a final dye concentration 2 μm for 1 min. After washed two times with serum-containing medium, cells were resuspend in 10 ml of KSR-medium for spheroid formation.

DETECTION OF HYPOXIA

The hypoxia probe LOX-1 (SCIVAX Co., Kanagawa, Japan) was used to demonstrate cellular hypoxia in spheroids or monolayer cultures. LOX-1 is a phosphorescent light-emitting iridium complex. Phosphorescence of LOX-1 is increased in response to low levels of oxygen which is detectable by a general fluorescent microscopy with excitation at 510–560 nm. Samples were incubated in medium containing 2 μM LOX-1 overnight at 37°C with a humid atmosphere of 5% CO_2. Phosphorescence of cultures was measured by the confocal laser scanning microscopy (LSM).

CELL DEATH DETERMINATION

Live and dead cells were detected with LIVE/DEAD® Cell Imaging Kit (488/570) (R37601, Invitrogen, Inc.) according to the manufacturer's protocol. The live cells were indentified with calcein AM which is non-fluorescent, cell permeant compound that is hydrolyzed by intracellular esterases into the fluorescent anion calcein. The dead cells were labeled with ethidium homodimer (EthD-1) which is a cell-impermeable dye for staining of dead and dying cells, which are characterized by compromised cell membranes. The images were observed and analyzed by LSM.

ALAMAR BLUE ASSAY

Cell viability was measured with AlamarBlue® (DAL1025, Invitrogen, Inc.) according the standard protocol. DPCs were seeded into the maintenance medium or KSR-medium at a density of 5×10^4 per ml. The cells were placed in 8 wells of 96-well plates and incubated for a total of 6 days. To measure cell proliferation, the seeded cells were incubated for 4 h with fresh culture medium supplemented with 10 vol.% AlamarBlue®. The AlamarBlue® reduction by the cells expressed as fluorescence intensity units was measured on a microplate reader (SH-9000Lab, HITACHI, Japan) with excitation 530 nm and emission 585 nm.

IMMUNOHISTOCHEMISTRY

Immunohistochemistry staining was performed with Histostain™ kit (Invitrogen, Inc.) according to manufactural protocol. Briefly, specimens were deparaffinized in xylene and dehydrated in a graded series of ethanol. The endogenous peroxidase activity was quenched by using 3% hydrogen peroxide in methanol. Specimens were incubated with serum blocking solution for 10 min to suppress non-specific binding of IgG, and then incubated for 60 min with saturating levels of primary antibodies. The primary antibodies used were: anti-STRO-1 (R&D Systems, MAB1038), anti-CD146 (Novocastra), anti-ki67 (Abcam, ab15580), anti-HuC/D (Invitrogen, Inc., A-21271), anti-Runx2 (Abcam, ab23981), anti-FGF3 (Abcam, ab103228), anti-FGF4 (Abcam, ab65974), and anti-P75 (Abcam, ab8874). For immunoperoxidase staining, specimens were reacted with biotinylated secondary antibody (provided from the kit) in dark for 10–20 min. The DAB then is used to create an intense red or brown deposit around the antigen/antibody/enzyme complex in the sample. For immunofluorescence staining, specimens were reacted with fluorochrome-conjugated secondary antibody (Invitrogen, Inc., A11001 or A11012) diluted to 2 μg/ml in PBS with 1.5% normal blocking serum. The nuclei were stained with DAPI. Images were taken by a bio-imaging navigator (Olympus, FSX100) and LSM.

Whole mount fluorescence immunohistochemical staining was performed with a standard protocol from http://www.abcam.com/. Samples were imaged and analyzed with LSM.

QUANTITATIVE REAL-TIME RT-PCR (qRT-PCR)

Total RNA was extracted from cultured spheroids and cell sheets using RNeasy Micro Kit (Qiagen, Tokyo, http://www1.qiagen.com) according to the manufacturer's protocol. RNA purity was evaluated by absorbance readings (Ratio A260/A230 and A260/A280) using the NanoDrop ND-1000 spectrophotometer (Thermo Fisher Scientific, Japan). Standard RT was performed to transcript RNA to cDNA using a High Capacity RNA-to-cDNA Master Mix kit (Applied Biosystems). The cDNA samples were subjected to qPCR amplification to analyze the selected genes, as well as *NFM*, *TUBB3*, *NANOG*, *CD24*, *CD44*, *CDH2*, *ITGB1*, *GLB1L2*, *TP63*, and *18S* (endogenous mRNA control). Human-specific probes for those genes were purchased from Applied Biosystems. PCR amplification mixture (20 μl) contained 2 μl single strand cDNA template, 10 μl TaqMan® Gene Expression Master Mix (Applied Biosystems) and 1 μl probe. Using standard curve method, we demonstrated that the relative efficiencies of target genes and 18s from each of the samples were approximately equal. Amplification reactions were run (in triplicate) on a StepOne Plus real-time PCR system (Applied Biosystems) using ΔΔCt method with the accompanying data analysis software.

HISTOLOGICAL ANALYSIS

The samples were fixed in 10% (v/v) buffered formalin for histological analyses. The specimens were embedded in paraffin, cut into about 5 μm thick sections, and then stained with Alizarin red S and light green for morphological analysis of mineralization.

QUANTITATION OF MINERALIZATION

We invent a novel method to quantify Alizarin red staining. After the cells or spheroids were stained with Alizarin red S (light green staining was omitted), 2 N NaOH/DMSO (1:1) was added to each culture well and shook for 10 min. The extract showed a purple color with an absorbance peak at 542 nm (Fig. 6D). The extract was immediately transferred to a 96-well plate and read for absorbance with a microplate reader (HITACHI, SH-9000Lab) at 542 nm.

STATISTICAL ANALYSIS

All data, expressed as mean ± standard deviation, were processed statistically by the software of SPSS11.5 for Windows. The differences of the data were considered especially when $P < 0.05$.

RESULTS

GENERATION OF SPHEROIDS FROM HUMAN DENTAL PULP CELLS BY KSR-MEDIUM

To generate spheroids, we used a serum-free medium containing a Knockout™ Serum Replacement (Invitrogen, Inc.) (KSR-medium) (Table I). We observed that under KSR-medium, DPCs spontaneously formed some spheroids whereas the other two types of cells, immortalized human periodontal ligament cell line, Pelt cells and oral epithelial cell line, NDUSD-1 cells, could not (Fig. 1B). About 70% of the spheroids adhered the culture surface with diameters from 100 to 200 μm, the rest 30% (diameters are over 200 μm) floated at the first 1–3 days, and then most of them adhered the culture surface later. Histological examination revealed a diversity of nuclei in the spheroid suggesting cells in the spheroid were multi-type (Fig. 1C, left). We transferred the floating spheroids to a new culture plate in KSR-medium, and found that these spheroids could preserve similar sizes for up to 107 days. When they have been further transferred into a serum-containing maintenance medium, those spheroids proliferated, indicating cells in the spheroids could survive more than 15 weeks (Fig. 1C, middle and right). Time-lapse video showed that Hoechest 33342-labeled cells in the spheroids in KSR-medium did not divide within 72 h (Fig. 1D and Movie S1). Hoechest 33342 tracking assay also showed that even after 5 weeks (4 weeks in KSR-medium + 1 week in maintenance medium) of cultivation, cells in the center of spheroids still stayed at resting stage with positive staining of a live cell marker Calcein AM (Fig. 1E).

We labeled DPCs with PKH26 (which interrupts the membrane integrity) in KSR-medium to form spheroids. As a result, DPCs only formed small sized spheroids (diameters are less than 100 μm). The spheroids were floated in the medium and died after 2 weeks of cultivation (Fig. S1). We also generated DPC spheroids in the low

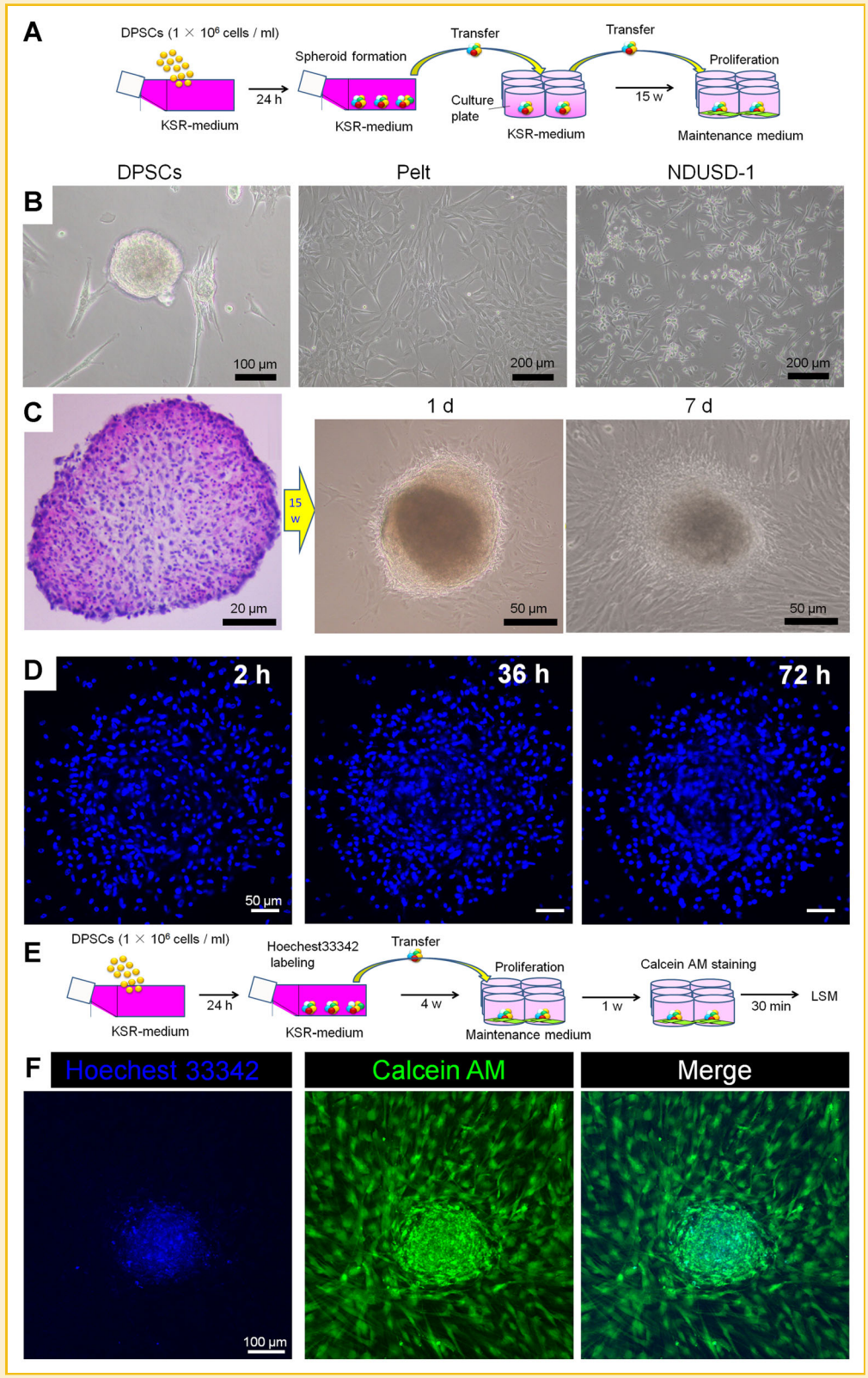

Fig. 1. Formation of DPCs-derived spheroids in KSR-medium. A: Experimental setup of (B) and (C). B: After being cultivated in KSR-medium for 24 h, DPCs formed spheroids (left). Pelt cells (middle) and NDUSD-1 cells (right) failed to form spheroids. C: HE staining of an 1-week spheroid. The spheroid showed a diversity of nuclei (left). After being transferred to maintenance medium for 1 day, a 15-week spheroid adhered to the culture surface (middle) and proliferated after 7 days (right) ($n = 5$). D: An 1-week spheroid was labeled with Hoechest 33342 and observed with LSM every hour for 72 h. The nuclei did not divide within 72 h ($n = 3$). See also time-lapse video in Movie S1. E: Experimental setup of (F). F: Cells in the center of the spheroid did not divide even after 5 weeks (4 weeks in KSR-medium + 1 week in maintenance medium) of cultivation. Cells in the spheroids are positive to calcein AM staining as well as the outside migrated cells indicating they are still alive.

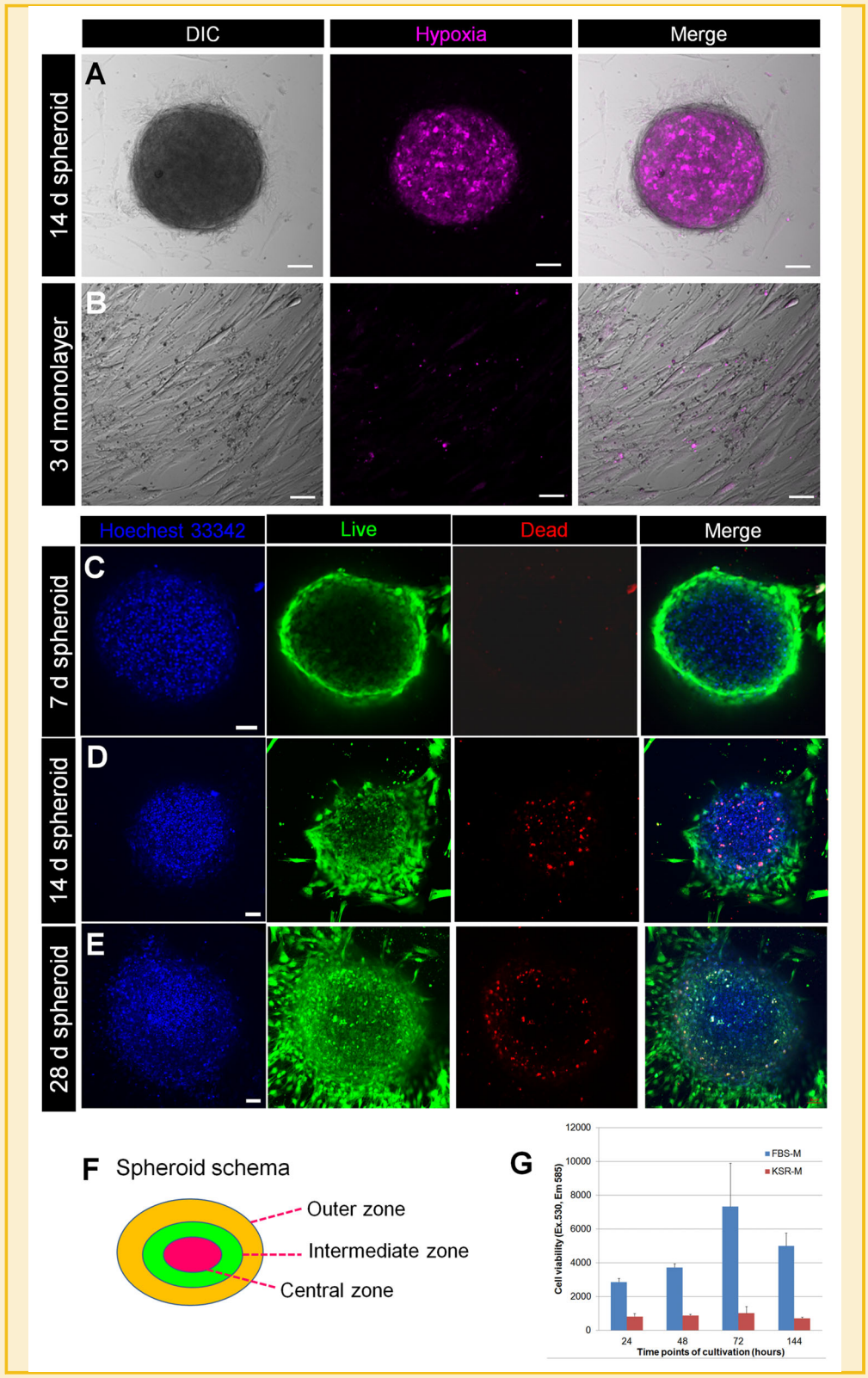

Fig. 2. Cellular hypoxia, nuclear dynamic, and cell death in spheroid in KSR-medium. Cellular hypoxia was detected with LOX-1 probe. A: Inside the spheroid LOX-1 probe emitted purple (pseudo color)-phosphorescence suggesting that cellular oxygen content was low ($n = 3$). Scale bar = 50 μm. B: LOX-1 probe was quenched by oxygen in the monolayer DPCs ($n = 3$). Scale bar = 50 μm. Cell death was measured with LIVE/DEAD staining in the 1- (C), 2- (D), and 4-week spheroids (E) ($n = 5$). For cell tracking, the nuclei were labeled with Hoechest 33342 1 day after spheroids formation. The intensity of Hoechest 33342-emitted fluorescence in the central and intermediate zones are almost the same among 7-, 14-, and 28-day spheroids. Scale bar = 50 μm. F: Schema of spheroid. G: Effect of KSR-medium on cell viability in DPCs. About 5,000 cells were seeded into 96-well plate in the maintenance medium or KSR-medium and incubated in general conditions. Cell viability was measured with alamar blue assay. FBS-M, maintenance medium; KRS-M, KSR-medium. Data represent the mean $\pm$ SD of three independent experiments.

adherent dish, with the result that all the spheroids floated in the culture media. After 2 weeks of cultivation, most of them decomposed, and left remnants of dead cells, cellular fragments, and debris (Fig. S2). These results suggested that the membrane integrity and cell adhesion are important to spheroid formation and long-term survival.

DETERMINATION OF HYPOXIA AND CELL DEATH IN SPHEROIDS

It has been reported that serum deprivation and hypoxia enhance stemness of human DPCs [Sakdee et al., 2009; Wang et al., 2010]. To discover if hypoxia occurs in the DPC-formed spheroids, we examined cellular oxygen level using LOX-1 probe. As shown in Figure 2A,B, compared to monolayer cultures, hypoxia wildly occurred inside the spheroids that indicated spheroids have much lower oxygen supply. We then detected cell death in the spheroids using LIVE/DEAD staining. The data showed that after 1 week of cultivation, very few dead cells occurred in the spheroid (Fig. 2C). Two weeks later, a little bit more cells underwent cell death (Fig. 2D). However, cell death did not markedly increase in the 4-week spheroids (Fig. 2E). Although some dead cells occurred in the central zone, most of them were distributed in the intermediate zone. Previous studies showed that starvation could cause mature cells to die but not a small population of stem cells [Angelo and Van Gilst, 2009] suggesting these dead cells in spheroid are probably mature cells. Hoechest 33342-labeled nuclei of the central and intermediate zones did not show any difference in fluorescent intensity among the 7-, 14-, and 28-day spheroids suggesting those cells have very slow cycling. Alamar blue assay showed that the cell viability of DPCs in KSR-medium maintained the same level during 6 days of cultivation confirming that DPCs did not grow (Fig. 2G). Because in vivo stem cells have infrequent cycling and reside in hypoxia microenvironment, we hypothesized that there were some stem cells in the center of spheroids.

STEM CELLS EXISTED IN THE CORE AND PROLIFERATIVE CELLS SHOWED IN THE MIDDLE

To confirm the above-mentioned hypothesis, we then tested the expression of stem cell markers by immunostaining and qRT-PCR. As

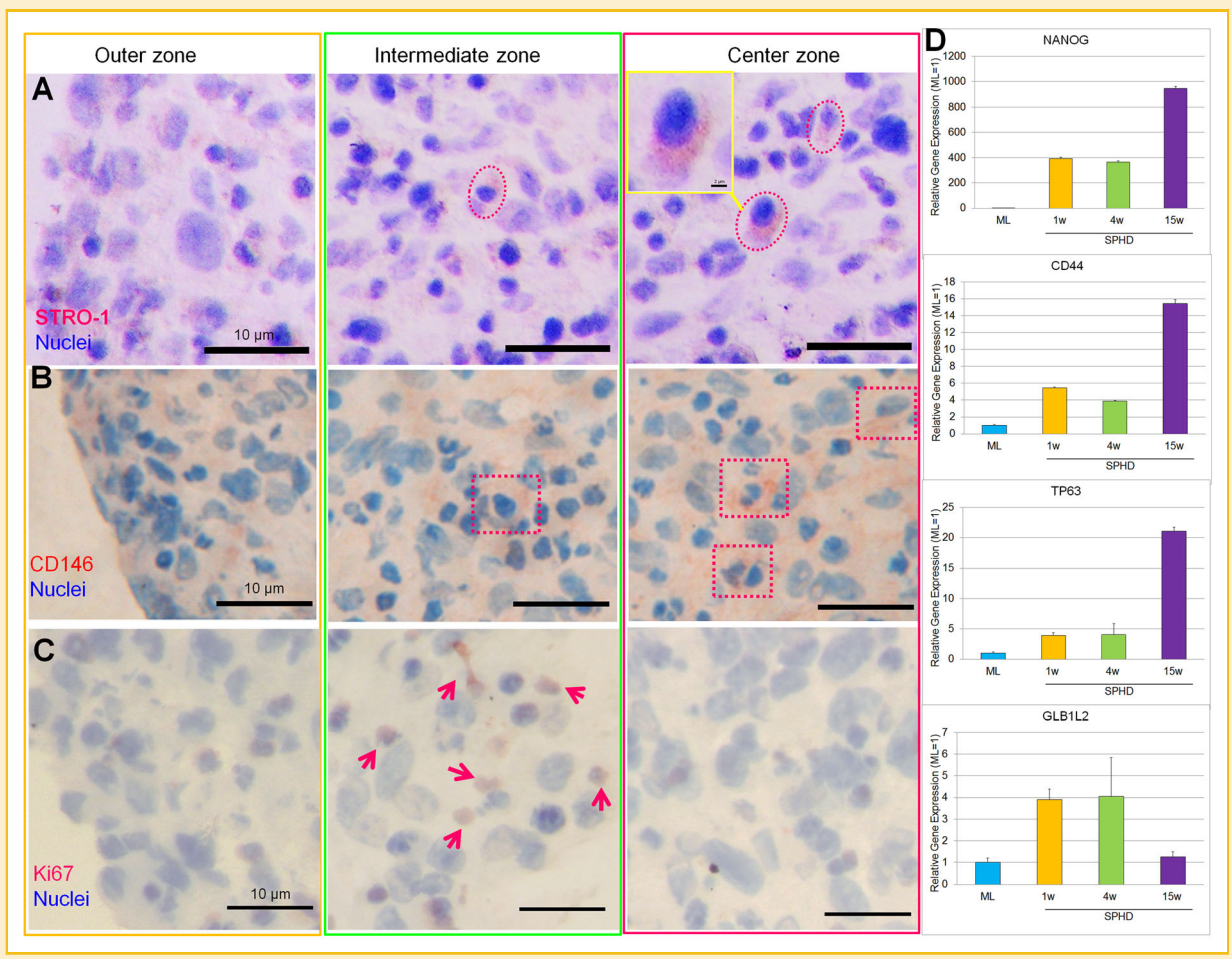

Fig. 3. Expression of stemness and proliferation markers in 4-week spheroids. The mesenchymal stem cells were identified by STRO-1 and CD146 antibodies by immunohistochemical staining. A,B: STRO-1(+) and CD146 (+) cells were observed both in the intermediate and central zones of spheroids (red dot cycles or squares). C: Cell proliferation of spheroids was determined by Ki67 antibody. The intermediate zone showed Ki67 (+) cells (red arrows). Nuclei were stained by hematoxylin ($n = 5$). D: Expression of stemness and senescence-associated markers in spheroids and 3 day monolayer DPCs was determined by qRT-PCR analysis. SPHD, spheroid; ML, 3 days monolayer DPCs. Data represent the mean ± SD of five independent experiments.

shown in Figure 3A,B, mesenchymal stem cell markers STRO-1 and CD146 were expressed in both central and intermediate zones of 4-week spheroids. The cells in the core showed strong expression of STRO-1. We also tested cell proliferation in the spheroids using Ki67 antibody by immunostaining. As shown in Figure 3C, in the intermediate zone of 4-week spheroids, Ki67 (+) cells were observed. The data demonstrated that cell proliferation also existed in the spheroids. To further confirm the distribution of stem cells and proliferative cells, we performed whole mount immunohistochemistry staining for Ki67 and STRO-1 with LSM. As shown in Figure 4A,B, Ki67 signals were detected mostly in the intermediate zone, and STRO-1 was expressed in both central and intermediate zones. Ki67 and STRO-1 were both absent in the surface and outer zone. Since dead cells also distributed in the intermediate zone, it is possible that

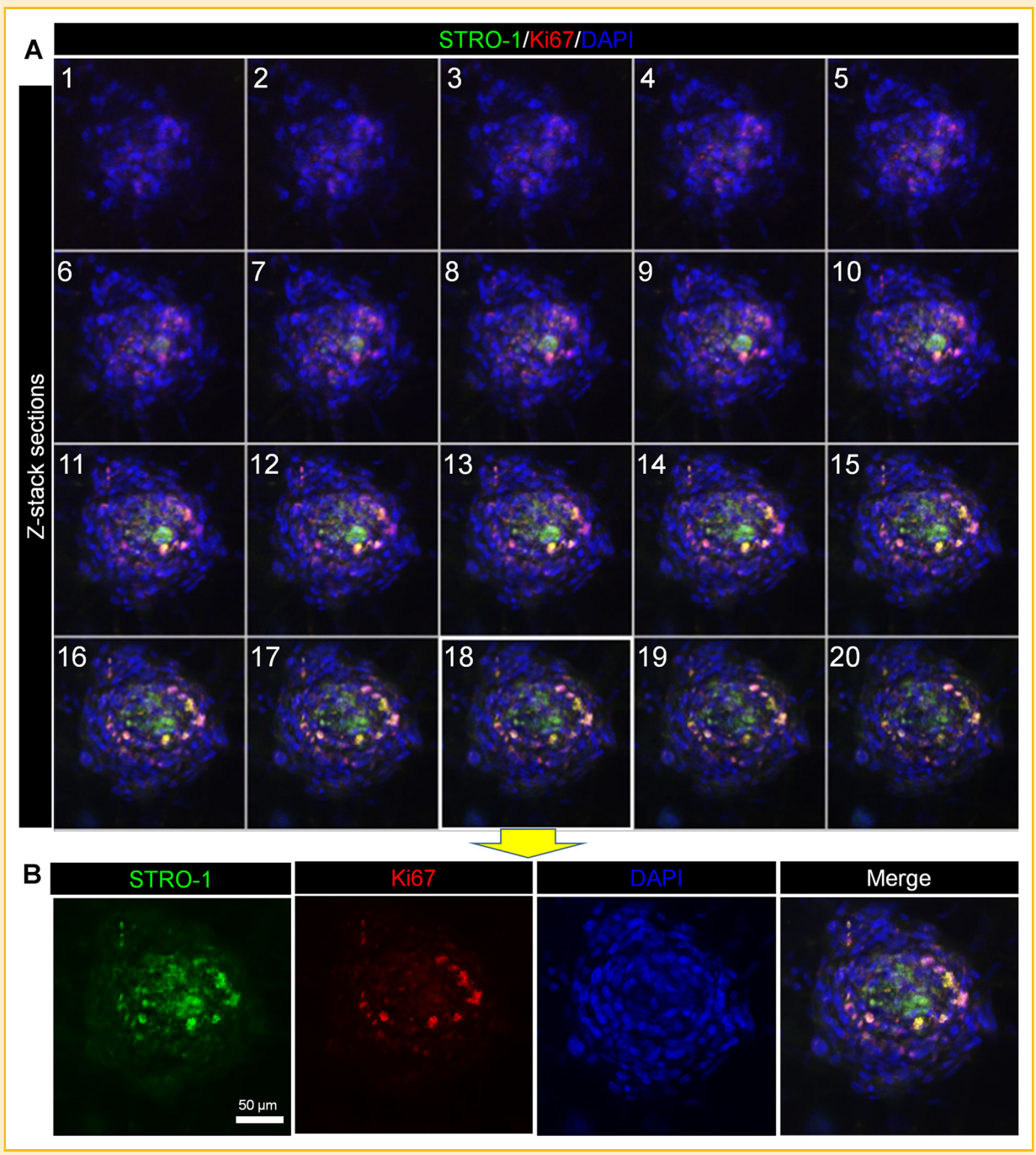

Fig. 4. Distribution of stem cells and proliferative cells in the spheroids. A: Whole mount immunohistochemistry staining for STRO-1 (green) and Ki67 (red) was performed on 4-week spheroids ($n = 3$). Z-series images were captured every 1.5 μm through the spheroid (30.1 μm in total). Representative sections demonstrate that the STRO-1 (+) cells distributed both in the intermediate and central zones, and the Ki67 (+) cells were most in the intermediate zone. B: Section No. 18 was split to three channels.

proliferative cells were there to cover the cell loss and then keep the homeostasis.

qRT-PCR analysis showed that, compared to monolayer DPCs, 1-, 4-, and 15-week spheroids showed much higher expression levels of stem cell markers, such as *NANOG*, *CD44*, and *TP63*. Especially, the 15-week spheroids showed the highest expression levels of those stemness markers suggesting that after long-term incubation in KSR-medium the stem cell rate increased. On the other hand, the senescence marker *GLB1L2* expressed at about the same level in spheroids and monolayer cells (Fig. 3D).

We then tested the expression of survival molecules FGF4 and FGF3 by immunofluorescence staining. Figure 5A shows that FGF4 molecules were expressed in the central zone and FGF3 molecules were expressed in both central and intermediate zones. The outer zone neither expressed FGF4 nor FGF3. This expression pattern is similar to stem cell markers STRO-1 and CD146 suggesting FGF signaling plays important roles on stem cell survival and maintenance.

Since cell–cell contact and intercellular adhesion in spheroids are much stronger than in monolayer cells [Desoize et al., 1998], and the expression of CD44 (which helps a spheroid cell line acquiring a resistance to integrin antibody induced apoptosis [Mooney et al., 1999]) is increased more than 15 times in the 15-week spheroids, we further measured the expression of intercellular adhesion molecules *CDH2* and *ITGB1* by qRT-PCR. As shown in Figure 5B, the expression of *CDH2* and *ITGB1* in the spheroids was higher than the monolayer cultures, and increased in a time-dependent manner suggesting they are involved in regulating cell survival in the spheroids.

NEURONAL POTENCY OF SPHEROIDS

Because dental pulp is derived from neural crest-derived ectomesenchyme, as we described in the introduction, and the expression of neural marker *CDH2* was increased more than 45 times in the 15-week spheroids, we hypothesized that there are some neuronal progenitors in the DPCs-derived spheroids. We first examined the expression of P75 neurotrophin receptor (a typical neural crest marker) and neuronal protein HuC/D in 1-week spheroids. Immunofluorescence staining showed that cells in the intermediate zone of spheroids expressed human neuronal protein HuC/D, while cells in the central zone expressed neurotrophin receptor P75 (Fig. 6B).

We then compared the expression of other neuronal markers *CD24*, *NFM*, and *TUBB3* among 3-day monolayer cells, 1-, 4-, and 15-week spheroids using qRT-PCR analysis. As shown in Figure 6C, compared to monolayer DPCs, the expression of *CD24*, *NFM*, and *TUBB3* in spheroids were much higher. Especially in 15-week spheroids, the expression of *CD24*, *NFM*, and *TUBB3* was about 168, 810, and 41 times higher than monolayer cells. Among 1-, 4-, and 15-week spheroids, the expression of neuronal markers were increased in a time-dependent manner.

NEURAL CONVERSION OF LONG TIME CULTURED SPHEROIDS

When the spheroids were cultivated in KSR-medium over 1 week, a few cells derived from them appeared neuron-like shape with positive

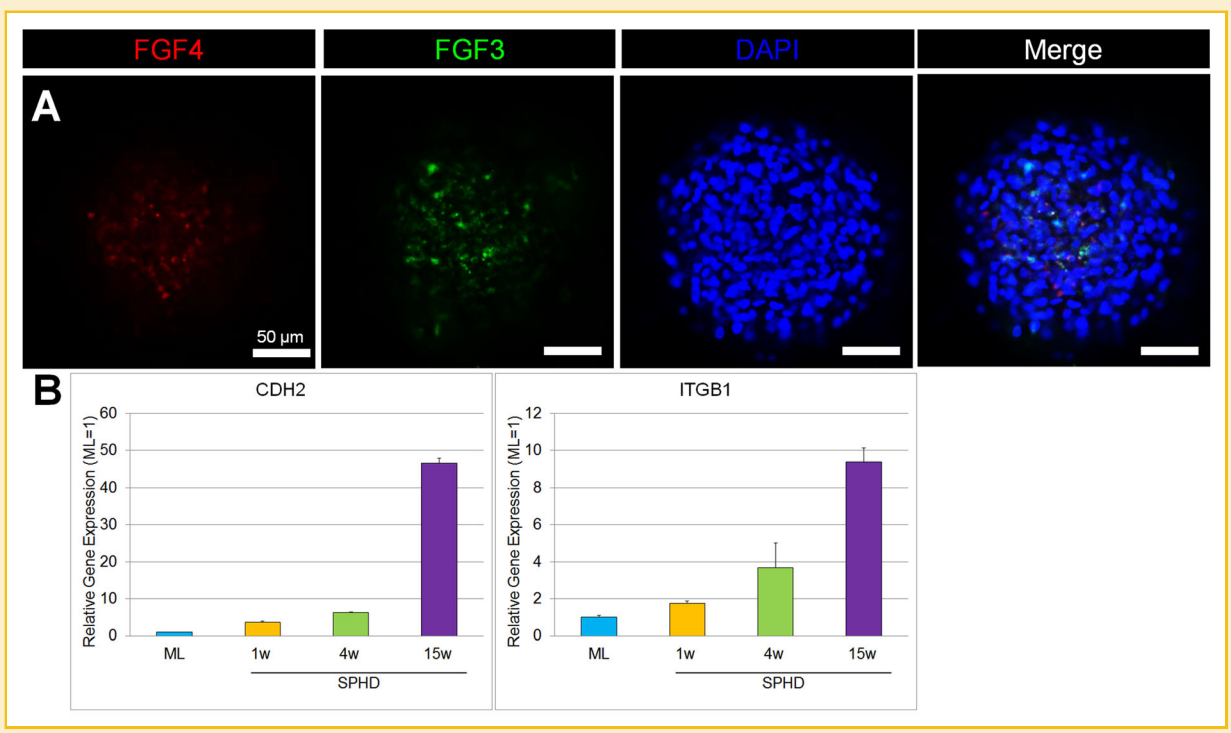

Fig. 5. Expression of cell survival-related molecules in spheroids. A: Cell survival markers FGF4 (red) and FGF3 (green) were co-expressed in the 4-week spheroid (n = 5). Scale bar = 100 μm. B: Comparison of markers for intercellular adhesion among 3-day monolayer cells, 1-, 4-, and 15-week spheroids by qRT-PCR analysis. SPHD, spheroid; ML, 3 days monolayer DPCs. Data represent the mean ± SD of five independent experiments.

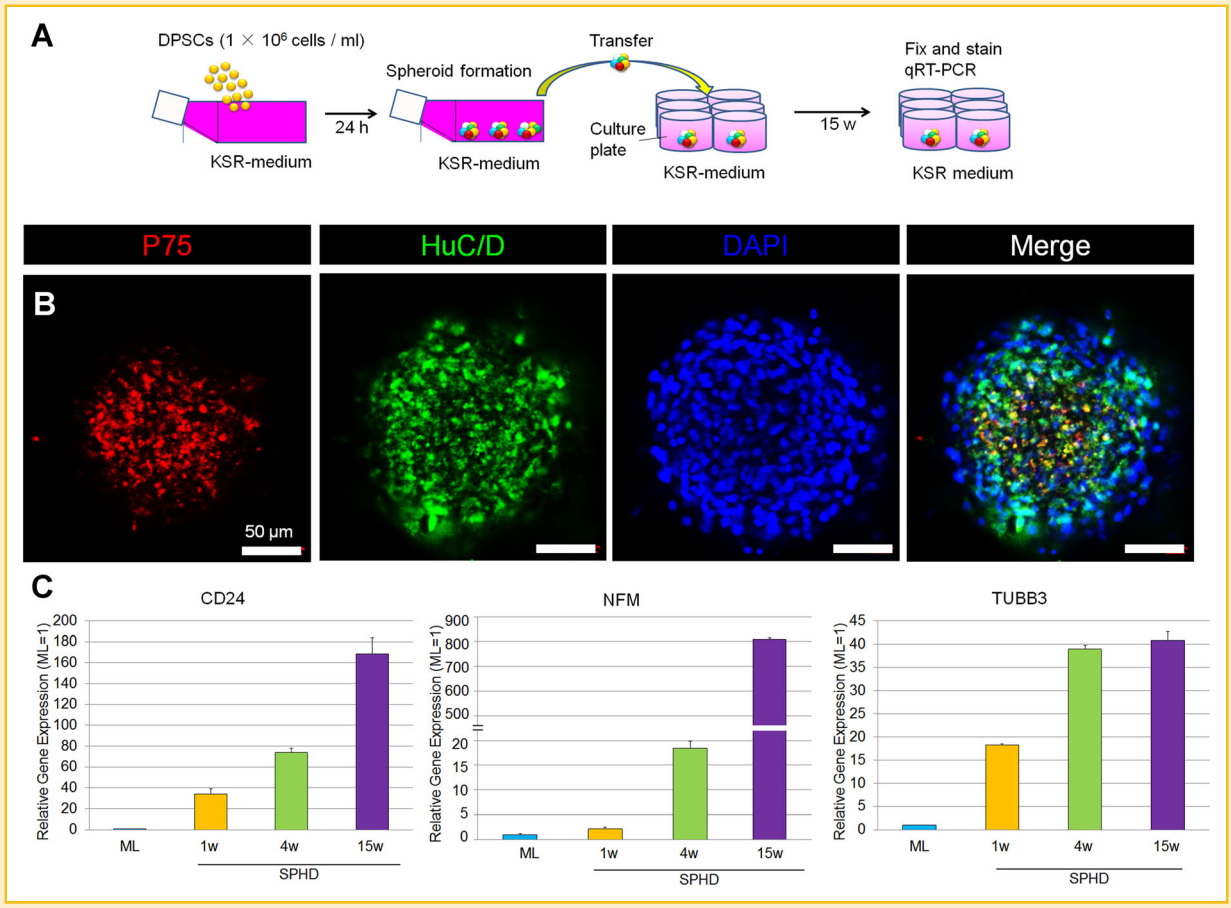

Fig. 6. Neuronal potential of spheroids. A: Experimental setup. B: Neural markers neurotrophin receptor P75 (red) and HuC/D (green) were co-expressed in 1-week spheroids ($n = 5$). C: Comparison of neural markers among 3-day monolayer cells, 1-, 4-, and 15-week spheroids by qRT-PCR analysis. Data represent the mean ± SD of five independent experiments.

expression of HuC/D and P75 proteins (Fig. 7B). To confirm where these neuron-like cells come from, we labeled the nuclei with Hoechest 33342 1 day after spheroid formation. As shown in Figure 7C, the cells inside the spheroids (which still have Hoechest 33342-emitted fluorescence indicating that they are the original cells) and the cells outside (which do not have Hoechest fluorescence indicating they are daughter cells) both expressed HuC/D and P75 (Fig. 7C). We also labeled the nuclei of monolayer DPCs and observed the expression of HuC/D and P75. The result showed that after 1-week cultivation monolayer DPCs divided several times thereby we could not detect the Hoechest 33342 signal. However, monolayer DPCs wildly expressed P75, and only few cells expressed HuC/D. The data suggested that cells in the spheroids could spontaneously differentiate into neural cells under KSR-medium.

OSTEO/ODONTOGENIC POTENTIAL OF SPHEROIDS

One important feature of pulp cells is their odontoblastic differentiation potency. We then differentiated spheroids by osteogenic medium (Table I). As shown in Figure 8, after 2 weeks of differentiation, cells inside the spheroids rapidly accumulated calcium and were positive to both Alizarin red and RUNX2/DSPP antibody-based immunofluorescence staining. Compared to the monolayer DPCs, mineralization in spheroids were significantly increased (Fig. 8C). Hoechest 33342-based cell tracking assay showed that cells inside the spheroids (the original cells) highly expressed DSPP confirmed that they are mature osteogenic/odontoblastic cells. RUNX2 was expressed in both the original cells and the daughter cells (Fig. 8D, upper panel). However, without differentiation, spheroids did not show positive staining to neither Alizarin red nor DSPP antibody in the maintenance medium. Only RUNX2 was weakly expressed in both original and daughter cells.

DISCUSSION

This study was initiated to characterize human DPCs-derived spheroids under a serum-free medium, KSR-medium. We demonstrated that under KSR-medium, only DPCs could form spheroids whereas other two types of cell, Pelt and NDUSD-1 cells could not. Cells in the spheroids have infrequent cycling and are surrounded by hypoxia microenvironment that is similar to the situation of adult stem cells in vivo. Because in some spheroids derived from cancer cells, lack of oxygen and nutrients causes central cell death [Desoize et al., 1998; Santini and Rainaldi, 1999; Bates et al., 2000], we needed

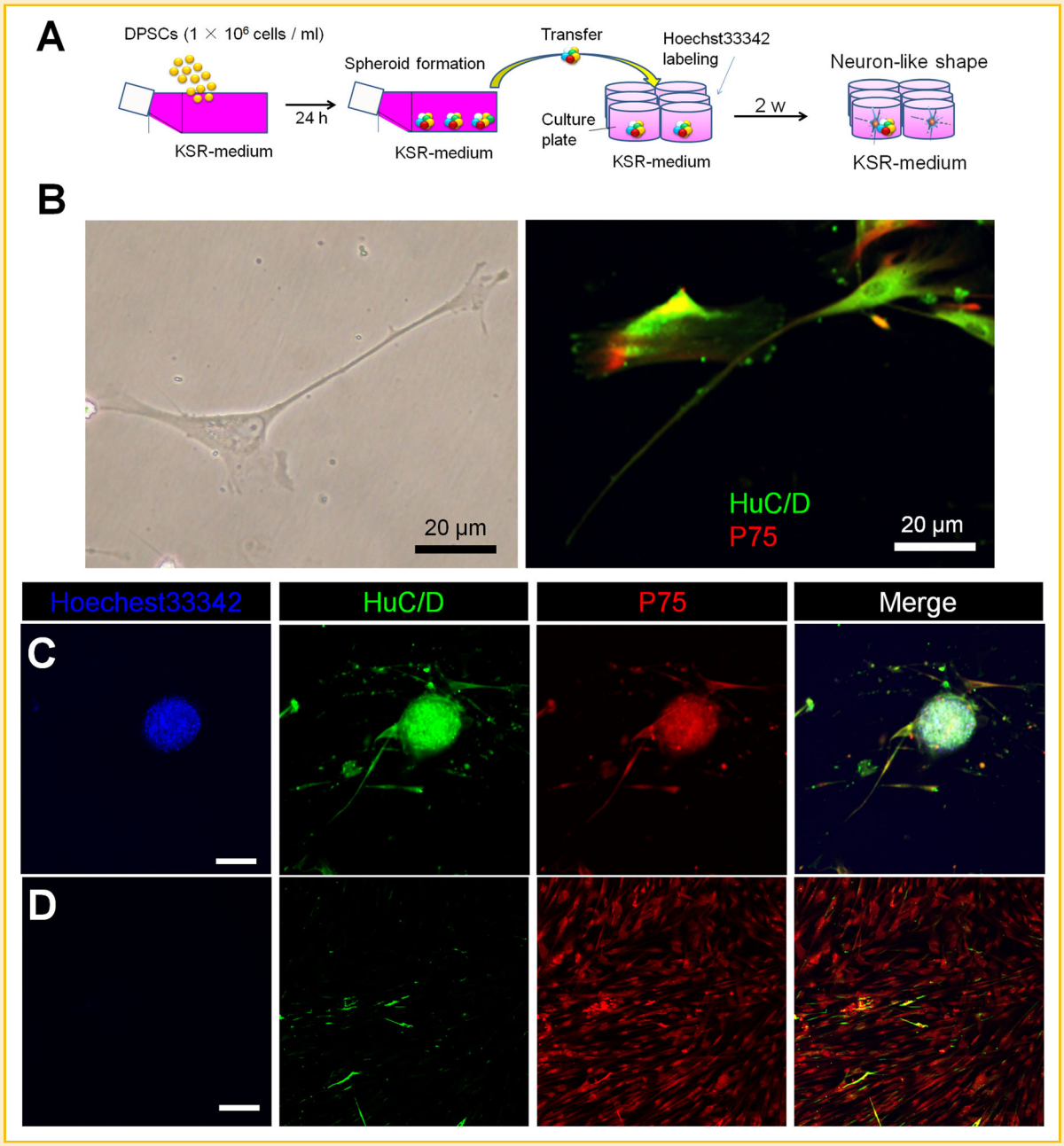

Fig. 7. Neural conversion of spheroids in KSR-medium. A: Experimental setup of (B) and (C). B: After 1 week of cultivation in KSR-medium, spheroid-derived cells appeared neuron-like shape, that show very thin and long cytoplasmic processes, resembling dendrites and axons (left). These cells co-expressed HuC/D and neurotrophin receptor P75 (right). C: Two-week spheroids and cells derived from them both expressed HuC/D and P75. Hoechest 33342-emitted fluorescence was only detected in the center of spheroids suggesting the outside neuron-like cells were not from the original cells but from divided daughter cells. Scale bar = 100 μm. D: Seven-day monolayer DPCs wildly expressed P75. Only few cells expressed HuC/D. The Hoechest 33342 signals could not be detected in the monolayer DPCs indicating these cells already divided server times (n = 3). Scale bar = 100 μm.

to clarify if cell death occurred in the center of the spheroid. LIVE/DEAD staining showed that cell death did not happen in the central zone but was limited in the intermediate zone of spheroids even after 4 weeks of cultivation in KSR-medium. Immunostaining confirmed that STRO-1 and CD146 were expressed mainly in the central zone indicating that mesenchymal stem cells were there. Interestingly, qRT-PCR analysis showed that after 15 weeks of cultivation in KSR-medium the stemness of spheroids was increased but the senescence kept the same. At the same time, neural markers *CD24*, *NFM*, and *TUBB3* were also increased in a time-dependent manner. The underlying mechanism for this observation can be explained as below: (1) at the beginning of cultivation, DPCs-derived spheroids contain various types of cells including stem cells, neural progenitors, and mature cells. During long-term cultivation, hypoxia and serum-free condition caused mature cells (they distributed in the intermediate zone) to die, but stem cells and neural progenitors

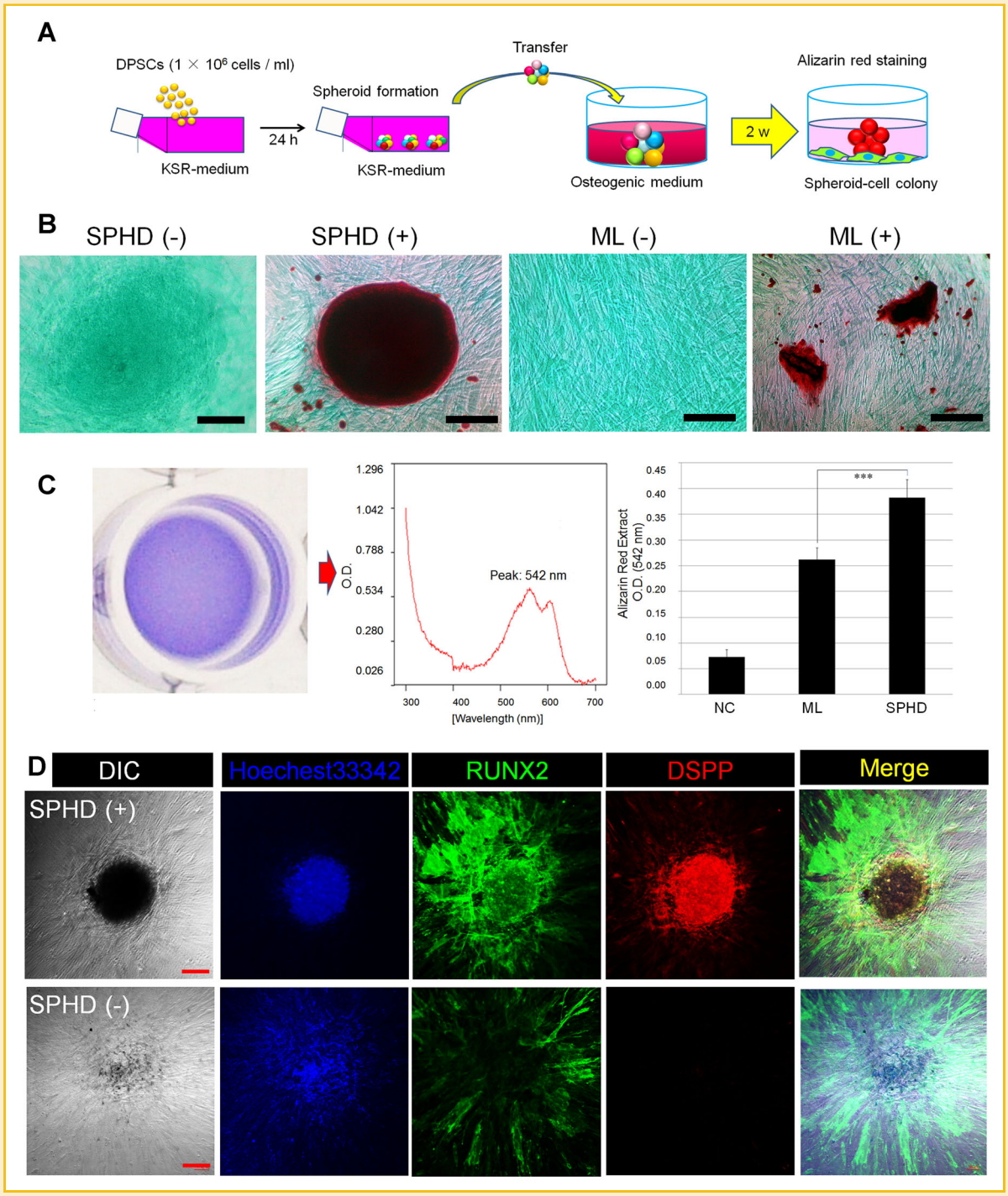

Fig. 8. Osteo/odontogenic differentiation of spheroids. A: Experimental setup. B: Spheroids and monolayer DPCs were underwent osteogenic differentiation for 2 weeks. Samples were then stained with Alizarin red S (red) and light green (green). SPHD (−), spheroids without differentiation (in the maintenance medium); SPHD (+), spheroids with differentiation; ML (−), monolayer without differentiation; ML (+), monolayer with differentiation ($n = 5$). Scale bar = 100 μm. C: To quantify alizarin red staining, 2 N NaOH/DMSO (1:1) was added to each well. The extract showed a purple color (left) with an absorbance peak at 542 nm (middle). Quantification of mineralization among negative control (NC), spheroids (SPHD) and monolayer (ML) cultures is shown in the right panel. $^{***}P < 0.001$. Data represent the mean ± SD of five independent experiments. D: Expression of osteo/odontogenic markers RUNX2 and DSPP in spheroids. Samples were treated as same as described in (B). The nuclei were labeled with Hoechest 33342 1 day after spheroids formation. In the spheroid with differentiation the original cells strongly expressed DSPP; and both the original cells and the daughter cells expressed RUNX2 ($n = 3$).

survived (hypoxia not only enhance stemness of human DPCs but also plays an important role in the maintenance of neural progenitors [Sakdee et al., 2009; De Filippis and Delia, 2011]). A recent study showed that for healing wounds, stem cells contribute substantially to the repair and long-term regeneration of the tissue, whereas committed progenitor cells make a limited contribution and died quickly [Mascré et al., 2012]; that partly confirmed our hypothesis. (2) It is also possible that mature cells were converted to stem cells or neural progenitors by the harsh environment. As mesenchymal stem cells can be generated from mature epithelial cells known as epithelial–mesenchymal transition (EMT), stemness may not be a fixed "immutable" state, but rather a more fluid existence [Alison et al., 2012] (Fig. S3).

Fibroblast growth factor (FGF) family possess broad mitogenic and cell survival activities and are involved in cell life-death-decisions, differentiation and proliferation. FGF4 and FGF3 are located closely on chromosome 11, and share similar functions on cell survival. FGF4 supports the undifferentiated growth of human embryonic stem cells and human bone marrow-derived mesenchymal stem cells, and maintains their pluripotency [Farré et al., 2007; Mayshar et al., 2008]. FGF3 signaling regulates proliferation and survival of neural progenitors [Kang et al., 2009]. Intercellular adhesion molecules, such as cadherins and integrins are important regulators of apoptosis, and controls self-renewal and pluripotency of human pluripotent stem cells [Li et al., 2012]. N-cadherin (CDH2) (also a neural marker) has been demonstrated involving in intercellular adhesion-dependent cell survival [Peluso et al., 1996; Lelièvre et al., 2012]. Integrin-β1 (ITGB1) signaling pathway not only provides an adhesive interaction but also regulates cell growth and prevents apoptosis [Gary and Mattson, 2001; Bouchard et al., 2008; Lawson et al., 2012]. Our data showed that FGF3 and FGF4 were expressed at both central and intermediate zone as same as the stem cells markers STRO-1 and CD146, and the expression of CDH2 and ITGB1 was increased in a time-dependent manner in spheroids suggesting FGF signaling and intercellular adhesion molecules likely played roles in stem cell survival.

Dental tissue has been considered as a source of neural crest stem cells (NCSCs) because DPCs share a common origin with neural crest cells. Our data showed that the expression of neural markers *CD24*, *NFM*, and *TUBB3* of the spheroids was increased in a time-dependent manner in KSR-medium. After 1-week cultivation in KSR-medium, cells in the spheroids spontaneously converted into neuron-like cells suggesting cells in the spheroids are akin to neural crest cells. Similar to our finding, other research group also observed that in the absence of serum dental ectomesenchymal stem cells can be cultured for long periods, and some cells showed neuron-like shape and expressed neural marker Nestin [Ibarretxe et al., 2012].

Dental pulp is an important source of ready-for-use autologous stem/progenitor cells for bone regeneration. A recent study showed that transplanted CD34 (+) pulp cells were able to regenerate a compact bone in human mandibles [Giuliani et al., 2013]. Previous studies demonstrated that DPSCs could produce mineralized nodes in both 2D monolayer culture system and scaffolds-based 3D culture systems. However, notable difference on mineralization between 2D and scaffolds-based 3D culture systems was not mentioned [Karbanová et al., 2010; Riccio et al., 2010; Atari et al., 2012; Cavalcanti et al., 2013]. The reason is considered that the scaffolds often do not provide a genuine 3D environment (cells grow on the scaffold surface that still keep the 2D manner), and cell–cell contact is not as tight as the spheroid model. Here we show that under osteogenic conditions, scaffolds-free 3D DPC-spheroids exhibited significantly higher efficacy than 2D monolayer DPCs on osteo/odontogeinc differentiation, especially the original cells of spheroid. This result suggests that 3D spheroid model can provide better microenvironment for mineralization than 2D culture. The data offer a possibility that DPC-spheroids might be a more convenient source for the therapy of bone defects.

This spheroid model helps us understand differentiation, tissue organization, and homeostasis of stem cells and offers wide applications in tissue regeneration, such as neural tissue and bone engineering.

ACKNOWLEDGMENTS

This work was supported in part by the Japan Society for the Promotion of Science (JSPS) Grant-in-Aid for Scientific Research (21890267 and 23592903). The authors would like to thank Mr. Nathaniel Green for proofreading.

REFERENCES

Abe S, Hamada K, Miura M, Yamaguchi S. 2012. Neural crest stem cell property of apical pulp cells derived from human developing tooth. Cell Biol Int 36:927–936.

Alison MR, Lin WR, Lim SM, Nicholson LJ. 2012. Cancer stem cells: In the line of fire. Cancer Treat Rev 38:589–598.

Angelo G, Van Gilst MR. 2009. Starvation protects germline stem cells and extends reproductive longevity in *C. elegans*. Science 326:954–958.

Arthur A, Rychkov G, Shi S, Koblar SA, Gronthos S. 2008. Adult human dental pulp stem cells differentiate toward functionally active neurons under appropriate environmental cues. Stem Cells 26:1787–1795.

Atari M, Caballé-Serrano J, Gil-Recio C, Giner-Delgado C, Martínez-Sarrà E, García-Fernández DA, Barajas M, Hernández-Alfaro F, Ferrés-Padró E, Giner-Tarrida L. 2012. The enhancement of osteogenesis through the use of dental pulp pluripotent stem cells in 3D. Bone 50:930–941.

Bates RC, Edwards NS, Yates JD. 2000. Spheroids and cell survival. Crit Rev Oncol Hematol 36:61–74.

Bouchard V, Harnois C, Demers MJ, Thibodeau S, Laquerre V, Gauthier R, Vézina A, Noël D, Fujita N, Tsuruo T, Arguin M, Vachon PH. 2008. B1 integrin/Fak/Src signaling in intestinal epithelial crypt cell survival: Integration of complex regulatory mechanisms. Apoptosis 13:531–542.

Cavalcanti BN, Zeitlin BD, Nör JE. 2013. A hydrogel scaffold that maintains viability and supports differentiation of dental pulp stem cells. Dent Mater 29:97–102.

Cotsarelis G, Cheng SZ, Dong G, Sun TT, Lavker RM. 1989. Existence of slow-cycling limbal epithelial basal cells that can be preferentially stimulated to proliferate: Implications on epithelial stem cells. Cell 57:201–209.

De Filippis L, Delia D. 2011. Hypoxia in the regulation of neural stem cells. Cell Mol Life Sci 68:2831–2844.

Desoize B, Gimonet D, Jardiller JC. 1998. Cell culture as spheroids: An approach to multicellular resistance. Anticancer Res 18:4147–4158.

Farré J, Roura S, Prat-Vidal C, Soler-Botija C, Llach A, Molina CE, Hove-Madsen L, Cairó JJ, Gòdia F, Bragós R, Cinca J, Bayes-Genis A. 2007. FGF-4 increases in vitro expansion rate of human adult bone marrow-derived mesenchymal stem cells. Growth Factors 25:71–76.

Fortunel N, Batard P, Hatzfeld A, Monier MN, Panterne B, Lebkowski J, Hatzfeld J. 1998. High proliferative potential-quiescent cells: A working model to study primitive quiescent hematopoietic cells. J Cell Sci 111:1867–1875.

Gary DS, Mattson MP. 2001. Integrin signaling via the PI3-kinase-Akt pathway increases neuronal resistance to glutamate-induced apoptosis. J Neurochem 76:1485–1496.

Giuliani A, Manescu A, Langer M, Rustichelli F, Desiderio V, Paino F, De Rosa A, Laino L, d'Aquino R, Tirino V, Papaccio G. 2013. Three years after transplants in human mandibles, histological and in-line holotomography revealed that stem cells regenerated a compact rather than a spongy bone: Biological and clinical implications. Stem Cells Transl Med 2:316–324.

Gronthos S, Mankani M, Brahim J, Robey PG, Shi S. 2000. Postnatal human dental pulp stem cells (DPCs) in vitro and in vivo. Proc Natl Acad Sci USA 97:13625–13630.

Huang GT, Gronthos S, Shi S. 2009. Mesenchymal stem cells derived from dental tissues vs. those from other sources: Their biology and role in regenerative medicine. J Dent Res 88:792–806.

Ibarretxe G, Crende O, Aurrekoetxea M, García-Murga V, Etxaniz J, Unda F. 2012. Neural crest stem cells from dental tissues: A new hope for dental and neural regeneration. Stem Cells Int 2012:103503.

Ishkitiev N, Yaegaki K, Imai T, Tanaka T, Nakahara T, Ishikawa H, Mitev V, Haapasalo M. 2012. High-purity hepatic lineage differentiated from dental pulp stem cells in serum-free medium. J Endod 38:475–480.

Kang W, Wong LC, Shi SH, Hébert JM. 2009. The transition from radial glial to intermediate progenitor cell is inhibited by FGF signaling during cortico-genesis. J Neurosci 29:14571–14580.

Kapur SK, Wang X, Shang H, Yun S, Li X, Feng G, Khurgel M, Katz AJ. 2012. Human adipose stem cells maintain proliferative, synthetic and multipotential properties when suspension cultured as self-assembling spheroids. Biofabri-cation doi: 10.1088/1758-5082/4/2/025004

Karbanová J, Soukup T, Suchánek J, Mokrý J. 2010. Osteogenic differentiation of human dental pulp-derived stem cells under various ex-vivo culture conditions. Acta Med (Hradec Kralove) 53:79–84.

Kubo C, Tsutsui TW, Tamura Y, Kumakura S, Tsutsui T. 2009. Immortalization of normal human gingival keratinocytes and cytological and cytogenetic characterization of the cells. Odontology 97:18–31.

Lawson MH, Cummings NM, Rassl DM, Vowler SL, Wickens M, Howat WJ, Brenton JD, Murphy G, Rintoul RC. 2012. Bcl-2 and β1-integrin predict survival in a tissue microarray of small cell lung cancer. Br J Cancer 103: 1710–1715.

Lelièvre EC, Plestant C, Boscher C, Wolff E, Mège RM, Birbes H. 2012. N-cadherin mediates neuronal cell survival through Bim down-regulation. PLoS ONE 7:e33206.

Li L, Bennett SA, Wang L. 2012. Role of E-cadherin and other cell adhesion molecules in survival and differentiation of human pluripotent stem cells. Cell Adh Migr 6:59–70.

Mannello F, Medda V, Tonti GA. 2011. Hypoxia and neural stem cells: From invertebrates to brain cancer stem cells. Int J Dev Biol 55:569–581.

Marga F, Neagu A, Kosztin I, Forgacs G. 2007. Developmental biology and tissue engineering. Birth Defects Res C Embryo Today 81:320–328.

Mascré G, Dekoninck S, Drogat B, Youssef KK, Brohée S, Sotiropoulou PA, Simons BD, Blanpain C. 2012. Distinct contribution of stem and progenitor cells to epidermal maintenance. Nature 489:257–262.

Mayshar Y, Rom E, Chumakov I, Kronman A, Yayon A, Benvenisty N. 2008. Fibroblast growth factor 4 and its novel splice isoform have opposing effects on the maintenance of human embryonic stem cell self-renewal. Stem Cells 26:767–774.

Mooney A, Jackson K, Bacon R, Streuli C, Edwards G, Bassuk J, Savill J. 1999. Type IV collagen and laminin regulate glomerular mesangial cell susceptibility to apoptosis via beta(1) integrin-mediated survival signals. Am J Pathol 155:599–606.

Nakamura T, Endo K, Kinoshita S. 2007. Identification of human oral keratinocyte stem/progenitor cells by neurotrophin receptor P75 and the role of neurotrophin/P75 signaling. Stem Cells 25:628–638.

Peluso JJ, Pappalardo A, Trolice MP. 1996. N-cadherin-mediated cell contact inhibits granulosa cell apoptosis in a progesterone-independent manner. Endocrinology 137:1196–1203.

Riccio M, Resca E, Maraldi T, Pisciotta A, Ferrari A, Bruzzesi G, De Pol A. 2010. Human dental pulp stem cells produce mineralized matrix in 2D and 3D cultures. Eur J Histochem 54:e46.

Sakdee JB, White RR, Pagonis TC, Hauschka PV. 2009. Hypoxia-amplified proliferation of human dental pulp cells. J Endod 35:818–823.

Santini MT, Rainaldi G. 1999. Three-dimensional spheroid model in tumor biology. Pathobiology 67:148–157.

Simon MC, Keith B. 2008. The role of oxygen availability in embryonic development and stem cell function. Nat Rev Mol Cell Biol 9:285–296.

Suda T, Takubo K, Semenza GL. 2011. Metabolic regulation of hematopoietic stem cells in the hypoxic niche. Cell Stem Cell 9:298–310.

Tsutsui T, Kumakura S, Yamamoto A, Kanai H, Tamura Y, Kato T, Anpo M, Tahara H, Barrett JC. 2002. Association of p16(INK4a) and pRb inactivation with immortalization of human cells. Carcinogenesis 23:2111–2117.

Vaheri A, Enzerink A, Räsänen K, Salmenperä P. 2009. Nemosis, a novel way of fibroblast activation, in inflammation and cancer. Exp Cell Res 315:1633–1638.

Wang W, Itaka K, Ohba S, Nishiyama N, Chung UI, Yamasaki Y, Kataoka K. 2009. 3D spheroid culture system on micropatterned substrates for improved differentiation efficiency of multipotent mesenchymal stem cells. Biomaterials 30:2705–2715.

Wang J, Wei X, Ling J, Huang Y, Gong Q. 2010. Side population increase after simulated transient ischemia in human dental pulp cell. J Endod 36:453–458.

Xiao L, Tsutsui T. 2012. Three-dimensional epithelial and mesenchymal cell co-cultures form early tooth epithelium invagination-like structures: Expres-sion patterns of relevant molecules. J Cell Biochem 113:1875–1885.

SUPPORTING INFORMATION

Additional supporting information may be found in the online version of this article at the publisher's web-site.

Fig. S1. Spheroid formation of PKH26-labeled DPCs in KSR-medium. A: Experimental setup. B: When DPSCs were labeled with PKH26 (a fluorescence dye which has long aliphatic tails can incorporate into lipid regions of the cell membrane), DPSCs only formed small sized spheroids in KSR-medium. Nuclei were stained with Heochest 33342. Scale bar = 20 μm.

Fig. S2. Spheroid formation on low adherent dish. A: Experimental setup. B: DPCs (1×10^6 cells/ml) were seeded in the low adherent dish. Twenty-four hours later, cells formed spheroids. C: HE staining of 1-week spheroids. The spheroids showed homogeneous nuclei (n = 3). D: Determination of cell death in spheroids by LIVE/DEAD® staining. Cell death massively happened in 1-week spheroids (n = 3). E: After been continually cultivated on the low adherent dish for about 2 weeks, most spheroids lost survival ability and became vestigial remnants.

Fig. S3. Hypothesis of cell fate in spheroid.

Movie S1. Spheroids were labeled with Hoechest 33342 and observed with LSM every hour for 72 h. The time-lapse video presented that cells inside the spheroids did not divide.